

Cell Reports

Supplemental Information

## **Genome-wide RNAi Screen**

# **Identifies Networks Involved in Intestinal Stem Cell Regulation in *Drosophila***

Xiankun Zeng, Lili Han, Shree Ram Singh, Hanhan Liu, Ralph A. Neumüller, Dong Yan,  
Yanhui Hu, Ying Liu, Wei Liu, Xinhua Lin, and Steven X. Hou

## SUPPLEMENTAL DATA

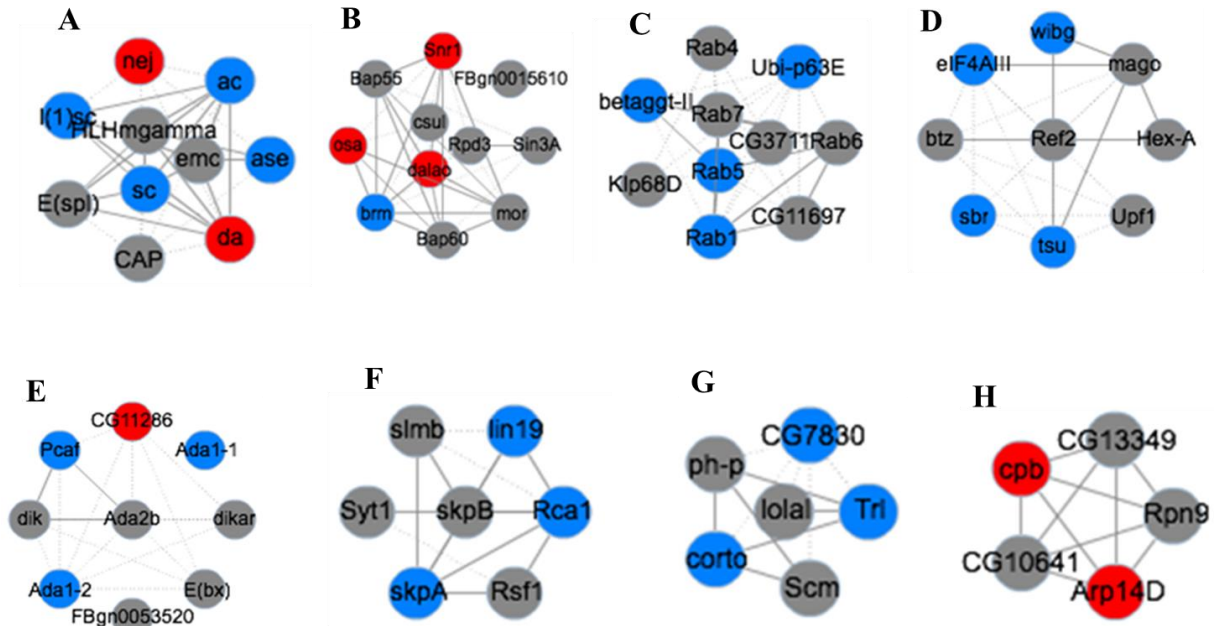


**Figure S1, Related to Figure 3. Representative Protein Complexes Identified Using COMPLEAT.**

(A) Transcription regulator complex. (B) Diagram of the Brm/Osa complex. (C) Endocytosis complex. (D) Pole plasm oskar mRNA localization complex. (E) Ada2p/Gcn5p/Ada3 transcription activator complex. (F) Ubiquitin-dependent protein catabolic process complex. (G) Chromatin silencing complex. (H) Regulation of actin polymerization or depolymerization. Red and blue are genes identified in the screen, grey are genes that are not identified in the screen but were identified by querying publicly available databases. The full list of protein complexes are shown in Table S3.

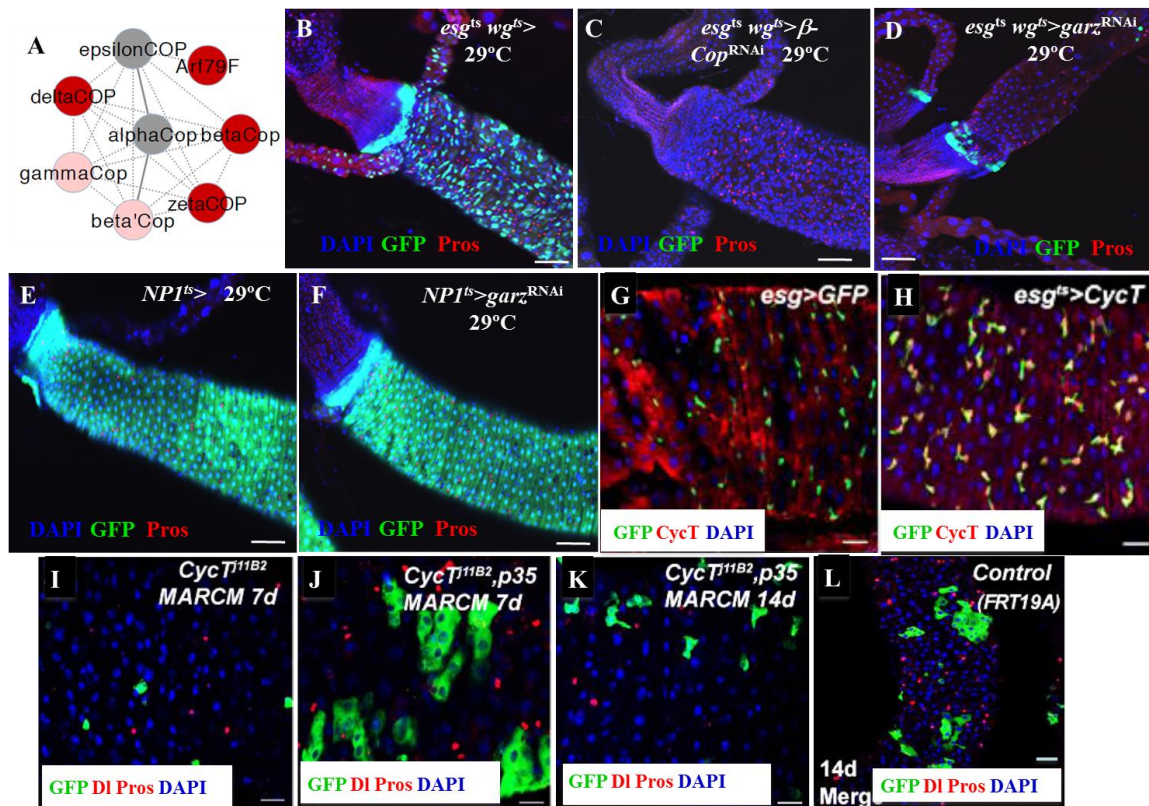


**Figure S2. (A-F) Related to Figure 2. Knockdowns of the COPI/Arf79F Complex Resulted in ISC Specific Cell Death.** (A) Diagram of the COPI complex. (B-D) Knockdowns of the COPI complex in the posterior midgut intestinal stem cells (ISCs) and hindgut intestinal stem cells (HISCs) using the *esg<sup>ts</sup> wg<sup>ts</sup>* double Gal4 (*UAS-mCD8.GFP; esg-Gal4 wg-Gal4; tub-Gal80<sup>ts</sup>*) resulted in stem cell death. (B) *esg<sup>ts</sup> wg<sup>ts</sup>* > control, (C) *esg<sup>ts</sup> wg<sup>ts</sup>* >  $\beta$ -*Cop*<sup>RNAi</sup>, (D) *esg<sup>ts</sup> wg<sup>ts</sup>* > *garz*<sup>RNAi</sup>, (E) *NPI<sup>ts</sup>* > (*UAS-mCD8.GFP; NPI-Gal4; tub-Gal80<sup>ts</sup>*) control, (F) *NPI<sup>ts</sup>* > *garz*<sup>RNAi</sup>. After cultured the flies at 29°C for 7 days, the posterior midguts of corresponding flies were dissected, stained with antibodies of GFP+DI+Pros+DAPI, and analyzed by confocal microscopy. Scale bars, 10  $\mu$ m.

**(G-L) Related to Figure 5. The CycT/Cdk9 Complex Regulates ISC Quiescent/Death.** (G) CycT protein expression in *esg* > *GFP* control flies. (H) CycT protein expression in *esg* > *CycT* flies. (I) *FRT<sup>79D</sup>-CycT<sup>j11B2</sup>* MARCM clones 7 days after clonal induction. (J) Expression of *p35* partially rescued the phenotype of *FRT<sup>79D</sup>-CycT<sup>j11B2</sup>* MARCM clones 7 days after clonal induction. (K) The rescued cells by expression of *p35* in *FRT<sup>79D</sup>-CycT<sup>j11B2</sup>* MARCM clones eventually died 14 days after clonal induction. (L) Control *FRT<sup>19A</sup>* MARCM clones 14 days after clonal induction. The posterior midguts of corresponding flies were dissected, stained with the indicated antibodies, and analyzed by confocal microscopy. Scale bars, 10  $\mu$ m.

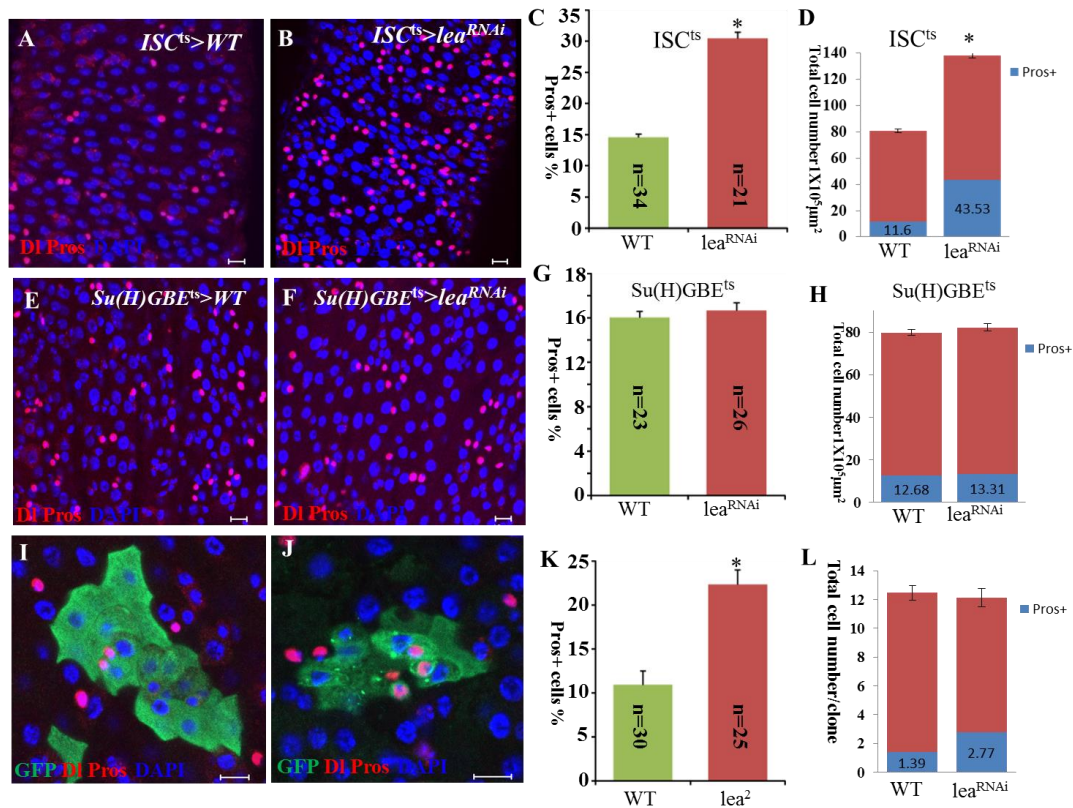


**Figure S3, Related to Figure 6. Robo2 Represses EE Cell Generation in ISCs.** (A–G) Knockdown of *lea* in ISCs ( $ISC^{ts}>lea^{RNAi}$ ;B), but not in EBs [ $Su(H)GBE^{ts}>lea^{RNAi}$ ;F], resulted in a significant increase the percentage of Pros+ EE cells, as compared with their wild-type counterparts (B compares with A; F compares with E). (C) The quantitative percentages of Pros+ cells among all cells in A and B. (D) The quantitative cell numbers (total Pros+ cells in blue box) in equal areas in A and B. (G) The quantitative percentages of Pros+ cells among all cells in E and F. (H) The quantitative cell numbers (total Pros+ cells in blue box) in equal areas in E and F. (I–L) MARCM clones of wild-type control (I) and *lea*<sup>2</sup> (J). Seven days after clone induction, the proportion of Pros+ EE cells is significantly higher in the GFP-marked clones of both *lea*<sup>2</sup> (J), as compared with its wild-type counterpart (I), while the clone sizes are similar. (K) The quantitative percentages of Pros+ cells in GFP+ cells in I and J. (L) The quantitative cell numbers (total Pros+ cells in blue box) per clone in I and J. The adult fly posterior midguts were stained with the indicated antibodies. Scale bars, 5 μm.



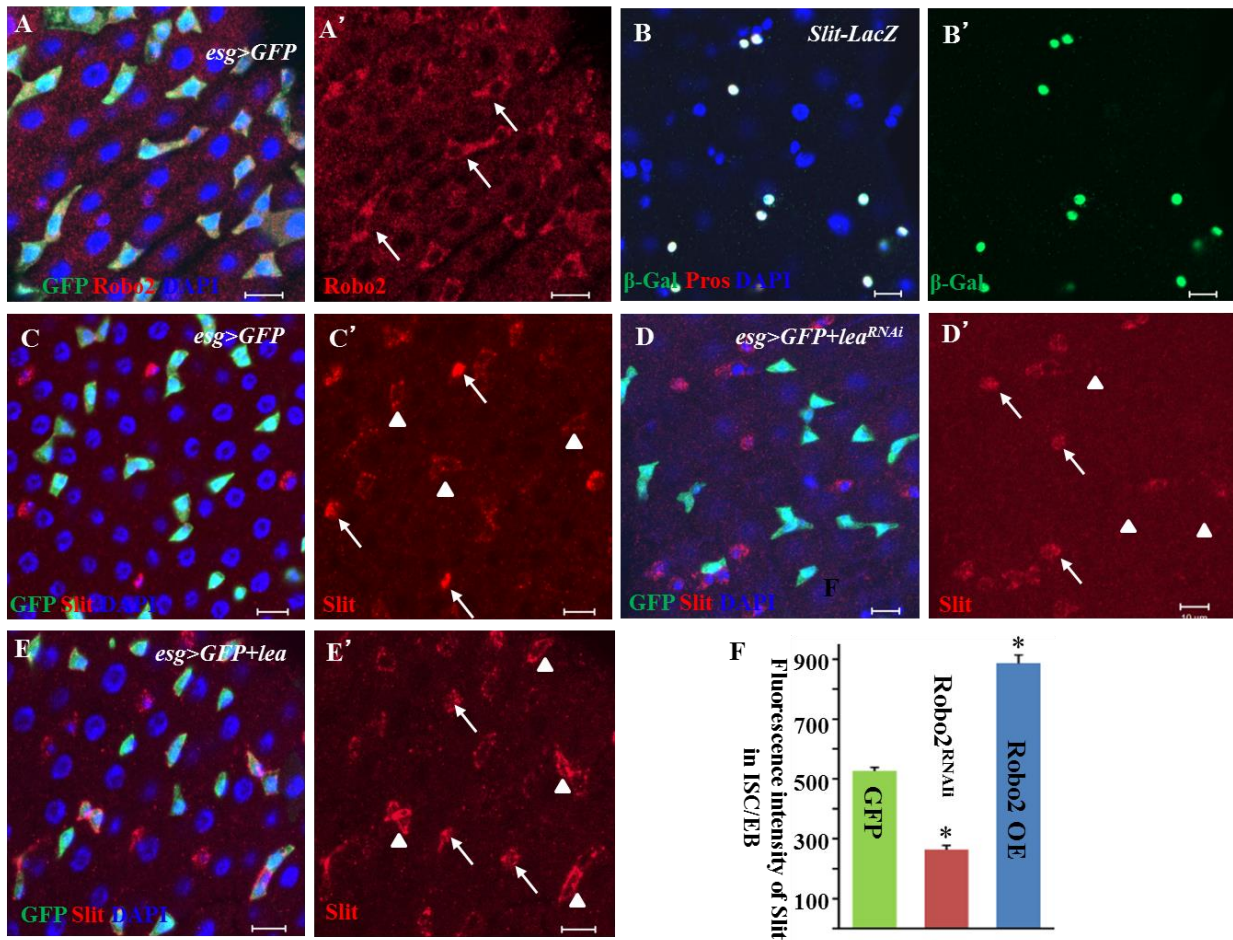


**Figure S4, Related to Figure 6. A Slit-Robo2 Signaling from EE cells to ISCs Regulates the Number of EE Cells through a negative feedback mechanism.**

(A, A') The Robo2 protein is expressed in mainly Esg-positive ISCs and Ebs (arrows in A'). (B, B') The *slit* gene is expressed mainly in EE cells (as detected by β-galactosidase in the *slit*<sup>PZ05248</sup> reporter line). (C, C') The Slit protein is strongly expressed in EE cells (arrows in C') and weakly expressed in the periphery of Esg-positive ISCs and EBs (arrowheads in C'). (D, D') Knockdown of *lea* (*esg >lea<sup>RNAi</sup>*) in ISCs and EBs is sufficient to reduce the amount of Slit protein near the periphery of these cells (arrowheads in D') without affecting its expression in EE cells (arrows in D'). (E, E') Overexpression of *Robo2/lea* (*esg >lea<sup>EP2582</sup>*) in ISCs and EBs is sufficient to increase the accumulation of Slit protein at the periphery of these cells (arrowheads in E') without affecting its expression in EE cells (arrows in E'). (F) Quantitation of Slit protein near the periphery of ISCs and EBs in C–E. Scale bars in all panels, 5 μm.

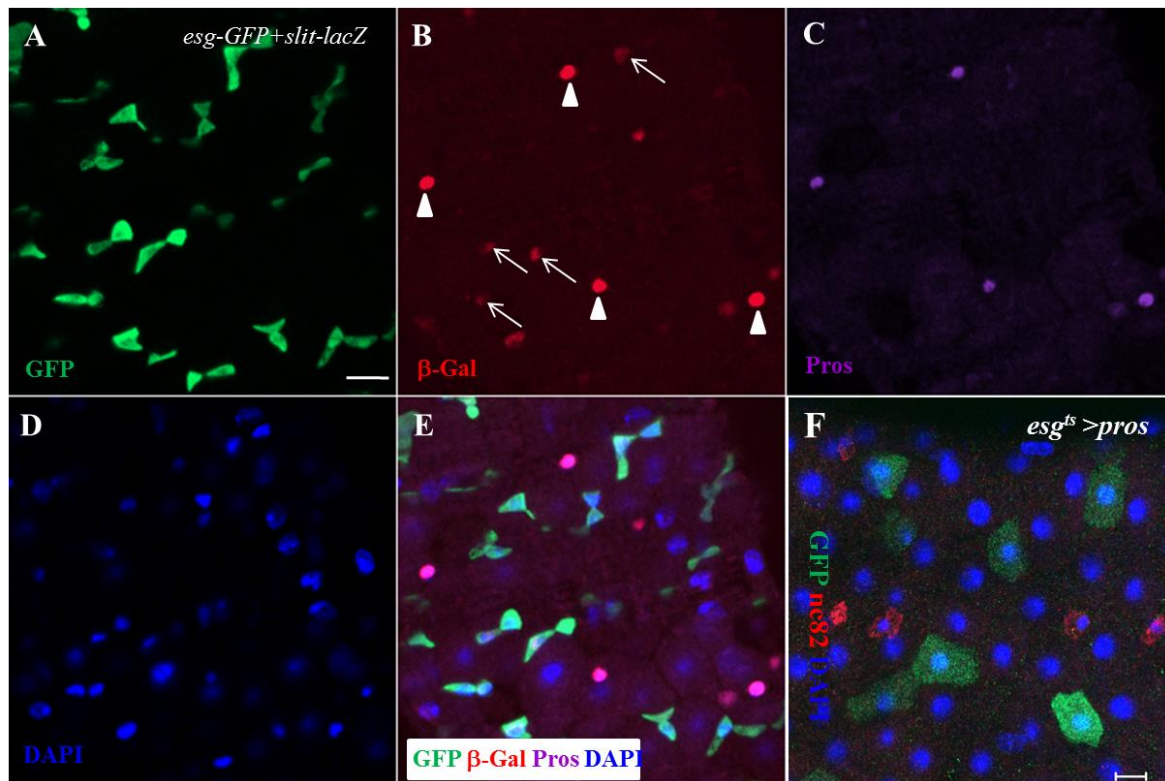


**Figure S5, Related to Figure 6. *slit* gene is strongly expressed in EEs and weakly in ISCs.**  
 (A-E) The *slit* gene is strongly expressed in EE cells (arrowheads in B) and weakly in ISCs (arrows in B).  
 (F) Overexpression of *pros* in ISCs (*ISC<sup>ts</sup>*>*pros*). The adult fly posterior midguts were stained with the indicated antibodies. Scale bars in all panels, 5 μm.

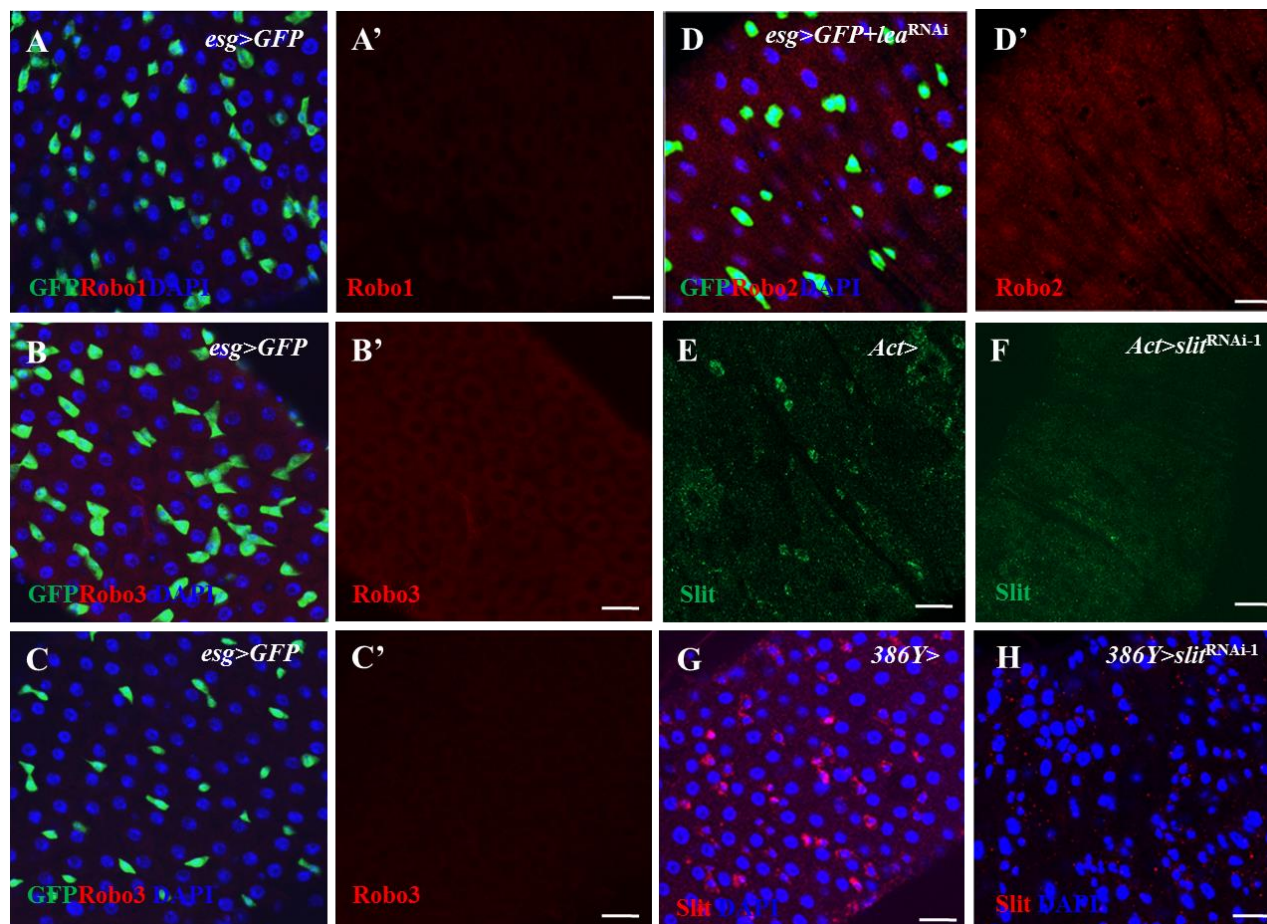


**Figure S6, Related to Figure 6. Expression of Robo1 and Robo3 and efficiency of *lea* and *slit* RNAi.** (A, A') The Robo1 protein is not detected in posterior midgut. (B-C') The Robo3 protein is not detected in posterior midgut. In B and B', mouse anti-Robo3 cytoplasmic (15H2) antibody was used. In C and C', mouse anti-Robo3 extracellular (14C9) antibody was used. (D, D') The Robo2 protein is effectively reduced in the *esg<sup>ts</sup>>lea<sup>RNAi</sup>* flies. (E, F) The Slit protein is effectively reduced in the *act<sup>ts</sup>>slit<sup>RNAi-1</sup>* flies. (G, H) The Slit protein is effectively reduced in the *386Y> slit<sup>RNAi-1</sup>* flies. The adult fly posterior midguts were stained with the indicated antibodies. Scale bars in all panels, 5  $\mu$ m.

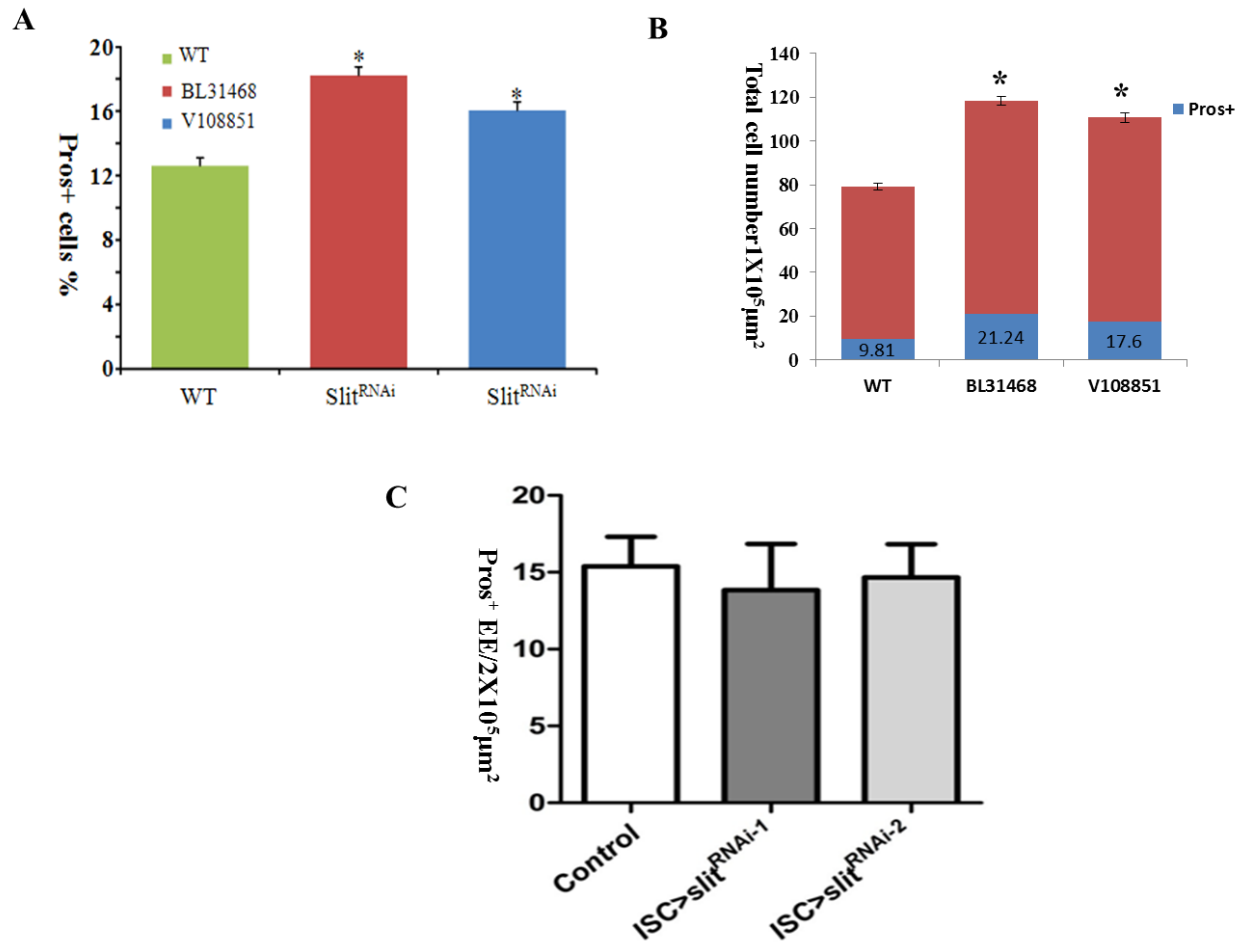


**Figure S7. Related to Figure 6. Knockdowns of *slit* in EEs rather than in ISCs affect EE numbers.** (A) Knockdown of *slit* in EE cells ( $386Y>slit^{RNAi}$ ) resulted in a small but significant increase the number of Pros+ EE cells, as compared with their wild-type counterparts. (B) The quantitative cell numbers (total Pros+ cells in blue box) in equal areas in A and B. (C) Knockdown of *slit* in ISCs ( $ISC^{ts}>slit^{RNAi}$ ) did not significantly affect the number of Pros+ EE cells, as compared with their wild-type counterparts. The wild type,  $386Y>slit^{RNAi}$ , and  $ISC^{ts}>slit^{RNAi}$  flies were stained using anti-Pros antibody after 14 days at 29°C.



## SUPPLEMENTAL EXPERIMENTAL PROCEDURES

### qPCR.

Total RNA from Act<sup>></sup>RNAi adult fly guts was isolated using the RNeasy™ Mini Kit (Qiagen) with on-column DNase digestion to remove genomic DNA. cDNA was synthesized using the ThermoScript™ RT-PCR System (Invitrogen). Real-time PCR analysis was performed on a real-time PCR system, Mastercycler Realplex (Eppendorf), using SYBR Green PCR Master Mix (Clontech). Primers were selected using FlyPrimer Bank.

### Bioinformatics analysis.

1. The ISC genetic network (Figure 3A) was generated as previously described in Yan et al 2014. In brief: The network was built by generating an interaction matrix using the following sources: protein-protein interactions (BioGrid, IntAct, MINT, DIP, DPiM and DroID (Sep 2012 version)), genetic interactions (FlyBase, BioGrid and DroID (Sep 2012 version)) and Literature cocitation interactions: gene2pubmed association was retrieved from NCBI EntrezGene ftp site (<ftp://ftp.ncbi.nlm.nih.gov/gene/DATA/>) on Jan 8th 2013. Pairwise gene co-citation relationships were extracted from PubMed. An interaction matrix was established amongst all genes that scored in the ISC screen and the resulting network was visualized using the Cytoscape software. Molecular complexes or groups of genes with the same function are outlined in black. Note: Genes that are not part of the interaction network are not displayed in the Figure.

2. Complex analysis: Complex analysis was done using COMPLEAT (<http://www.flyrnai.org/compleat/>), a tool that annotates protein complexes from both literature and predictions from protein-protein network, and does gene set enrichment analysis based on protein complexes. Using COMPLEAT, we identified 79 non-redundant protein complexes that are over-represented among the genes scored comparing to the experimental background with p value cut-off 0.05 (Table S3).

3. ISC, Nb, and female GSC comparison (Figure 7B) and GO enrichment heatmap (Figure 7A).

GO term enrichment was performed with DAVID (<http://david.abcc.ncifcrf.gov>) for ISC, GSC and Nb screens.